Susceptibility to kidney fibrosis in mice is associated with early growth response-2 protein and tissue inhibitor of metalloproteinase-1 expression

OPEN

Gábor Kökény[1,2], Ágnes Németh[1,2], Jeffrey B. Kopp[3], Weiping Chen[4], Andrew J. Oler[5], Anna Manzéger[1,2], László Rosivall[1,2] and Miklós M. Mózes[1,2]

[1]*Institute of Translational Medicine, Semmelweis University, Budapest, Hungary;* [2]*International Nephrology Research and Training Center, Semmelweis University, Budapest;* [3]*Kidney Disease Section, National Institute of Diabetes and Digestive and Kidney Diseases (NIDDK), National Institutes of Health (NIH), Bethesda, Maryland, USA;* [4]*Genomics Core Facility, National Institute of Diabetes and Digestive and Kidney Diseases (NIDDK), National Institutes of Health (NIH), Bethesda, Maryland, USA; and* [5]*Bioinformatics and Computational Biosciences Branch, Office of Cyber Infrastructure and Computational Biology, National Institute of Allergy and Infectious Diseases, National Institutes of Health (NIH), Bethesda, Maryland, USA*

Patients with chronic kidney disease and experimental animal models of kidney fibrosis manifest diverse progression rates. Genetic susceptibility may contribute to this diversity, but the causes remain largely unknown. We have previously described kidney fibrosis with a mild or severe phenotype in mice expressing transforming growth factor-beta1 (TGF-β1) under the control of a mouse albumin promoter (Alb/TGF-β1), on a mixed genetic background with CBAxC57Bl6 mice. Here, we aimed to examine how genetic background may influence kidney fibrosis in TGF-β1 transgenic mice, and in the unilateral ureteral obstruction (UUO) and subtotal nephrectomy (SNX) mouse models. Congenic C57Bl6(B6)-TGFβ and CBAxB6-TGFβ (F1) transgenic mice were generated and survival, proteinuria, kidney histology, transcriptome and protein expressions were analyzed. We investigated the kidneys of B6 and CBA mice subjected to UUO and SNX, and the effects of tissue inhibitor of matrix metalloproteinase-1 (TIMP-1) neutralization on the fibrotic process. CBAxB6-TGFβ mice developed severe kidney fibrosis and premature death, while B6-TGF-β mice had mild fibrosis and prolonged survival. Kidney early growth response factor-2 (EGR2) and TIMP-1 expression were induced only in CBAxB6-TGFβ mice. Similar strain-dependent early changes in EGR2 and TIMP-1 of mice subjected to UUO or SNX were observed. TIMP-1 neutralization *in vivo* hindered fibrosis both in transgenic mice and the SNX model. EGR2 over-expression in cultured HEK293 cells induced TIMP-1 while EGR2 silencing hindered TGF-β induced TIMP-1 production in HK-2 cells and ureteral obstructed kidneys. Finally, EGR2 and TIMP1 was increased in human kidneys manifesting focal segmental glomerulosclerosis suggesting a correlation between animal studies and patient clinical settings. Thus, our observations demonstrate a strong relationship between genetic background and the progression of kidney fibrosis, which might involve early altered EGR2 and TIMP-1 response, but the relationship to patient genetics remains to be explored.

Correspondence: *Gábor Kökény, Semmelweis University, Institute of Translational Medicine, Nagyvárad tér 4, H-1089 Budapest, Hungary. E-mail: kokeny.gabor@med.semmelweis-univ.hu*

Received 4 August 2021; revised 2 March 2022; accepted 30 March 2022; published online 2 May 2022

Kidney International (2022) **102,** 337–354; https://doi.org/10.1016/j.kint.2022.03.029

KEYWORDS: chronic kidney disease; fibrosis; focal segmental glomerulosclerosis; gene expression; proteinuria; transcription regulation

Translational Statement

Patients with chronic kidney disease, regardless of etiology, develop kidney fibrosis, but they manifest varying rates of progressive loss of kidney function. Moreover, ongoing kidney fibrosis is a major therapeutic challenge in nephrology. Differences in genetic susceptibility may contribute to differences in progression rates, driven by as-yet-unknown molecular mechanisms. In the present study, we addressed the question of whether genetic background affects the development and progression of kidney disease in several mouse models of renal fibrosis. We found that kidney fibrosis progression is strongly associated with mouse genetic background. This genetic susceptibility involves very early and marked overproduction of tissue inhibitor of matrix metalloproteinase-1 (TIMP-1), which is associated with early growth response factor-2 *in vivo* and *in vitro*. Further, we observed similar expression patterns in human renal biopsies manifesting focal segmental glomerulosclerosis. These results may help clarify the initial molecular mechanisms of kidney fibrosis and might lead to identification of early diagnostic markers and the development of pharmacologic inhibitors to slow, halt, or even reverse the fibrotic process.

Progressive kidney fibrosis, which often eventuates in end-stage kidney disease, is the final common pathway of chronic renal diseases of different etiologies, and it is one of the major challenges in nephrology. Patients with one particular renal disease, such as diabetic nephropathy or

arterionephrosclerosis (often previously misattributed to hypertension in the case of African Americans), show different progression rates, presumably due to genetic susceptibility.[1]

Transforming growth factor-beta1 (TGF-β1) is a multifunctional cytokine that regulates the dynamic balance of extracellular matrix components and affects cell growth and differentiation. TGF-β1 plays a pivotal role in not only the pathogenesis of fibrosis, but also development, wound healing, immune processes, and carcinogenesis. Experimental overexpression of TGF-β1 is associated with kidney,[2] myocardial,[3] pulmonary,[4] and hepatic fibrosis.

Several lines of evidence suggest a role for strain-dependent differences in the development and progression of experimental renal diseases. Rat models of puromycin aminonucleoside nephrosis and subtotal nephrectomy[5–7] have demonstrated the importance of strain differences. Studies involving albumin overload,[8,9] subtotal nephrectomy,[10,11] and diabetic nephropathy[12] mouse models show that the C57Bl6/J (B6) strain is more resistant to kidney fibrosis, compared to other mouse strains, including 129Sv, Balb/C, and DBA/2. Furthermore, despite early renal TGF-β1 overexpression after injury, B6 mice are resistant to fibrosis induced by renal ablation.[10,13] Important to note is that the molecular mechanisms underlying strain-dependent renal fibrosis remain largely unknown.

We examined the role of genetic background on the progression of TGF-β1–induced renal fibrosis in transgenic mice overexpressing TGF-β1.[14] Originally, TGF-β1 transgenic mice maintained on mixed (CBAxB6) genetic background developed progressive renal fibrosis with phenotypic variability, characterized as either mild or severe.[15] Therefore, we generated congenic B6-TGFβ transgenic mice that manifested only a mild renal phenotype, and CBAxB6-TGFβ F1 mice that had severe proteinuria and glomerulosclerosis, in order to analyze the expression of various fibrosis-related molecules in these transgenic strains. Further, we made similar inter-strain comparisons in the unilateral ureter obstruction (UUO) and subtotal renal ablation (SNX) models, complemented with cell culture studies and analysis of human focal segmental glomerulosclerosis (FSGS) kidney biopsies.

Our experimental data show that genetic background and progression of TGF-β1–induced renal fibrosis strongly correlate with altered tissue inhibitor of matrix metalloproteinase-1 (TIMP-1) expression, which is associated with early response of early growth response factor-2 (EGR2). We suggest that the underlying mechanism of resistance to renal fibrosis in B6 mice might involve the lack of early EGR2 and TIMP-1 response.

METHODS

Concise methods are provided in the Supplementary Methods.

RESULTS

Characterization of novel congenic B6–TGF-β1 transgenic mice

In order to confirm the role of genetic background on kidney fibrosis progression in this model, male CBA.B6-Alb/TGF-β_1 transgenic mice were backcrossed to both C57Bl6 (B6) and CBA inbred strains, as a CBAxB6 F1 hybrid mouse was the founder of this transgenic line.

The backcrossing of Alb/TGF-β_1 transgenic mice to the CBA strain failed, as 70% of the CBAxB6-TGFβ F1 males died before reaching 6 weeks of age (Figure 1a; Supplementary Figure S1A). In contrast, backcrossing of Alb/TGF-β_1 transgenic mice for 22 generations to the B6 strain greatly increased survival, compared with that in the original transgenic strain, which exhibited 100% mortality by age 52 weeks. We found that 72% of B6-TGFβ mice survived to age 15 weeks (Figure 1a), and at 52 weeks, 39% were alive, compared to 100% of B6 wild type controls ($n = 33$, log-rank test, $P < 0.001$).

At the age of 4 and 9 months, plasma TGF-β1 levels were 2-fold higher in B6-TGFβ transgenic mice, compared with levels in age-matched B6 controls (Supplementary Table S1). Body weights of both B6 and B6-TGFβ mice increased comparably with age (Supplementary Table S1). No differences were seen in kidney weights normalized to body weight, or in urinary protein-to-creatinine ratios among the groups. We observed mild but significant glomerulosclerosis in B6-TGFβ kidneys at ages 4 and 9 months, compared with age-matched B6 controls (Supplementary Table S1; Supplementary Figure S1B). We did not observe tubulointerstitial damage in B6–TGF-β1 mice at any of the ages investigated.

Proteinuria and shortened survival of novel CBAxB6-TGFβ F1 transgenic mice despite comparable plasma TGF-β1 levels

Plasma levels of TGF-β1 at age 14 days in B6-TGFβ and CBAxB6-TGFβ F1 mice were similar, and they were 11–14-fold higher than those in controls (Table 1). Body weights of transgenic mice were similar to their wild-type control (Table 1). In contrast to B6-TGFβ mice, the survival time of CBAxB6-TGFβ F1 mice was dramatically shorter, as only 60% of these F1 mice survived to age 2 weeks, and all mice died by age 12 weeks (Figure 1a). Despite comparable plasma TGF-β1 levels in B6-TGFβ and CBAxB6-TGFβ strains, only CBAxB6-TGFβ mice had significantly elevated urine protein-to-creatinine ratio (Figure 1b). Similarly, kidney weights and levels of serum urea were significantly higher only in CBAxB6-TGFβ F1 mice (Figure 1c). Due to the early uremic death of most CBAxB6-TGFβ F1 mice, we were not able to continue the backcross to the CBA strain, and all experimental samples were obtained at age 14 days.

Onset and progression of kidney fibrosis in TGF-β_1 transgenic mice is strain-dependent

At 14 days of age, B6-TGFβ mice exhibited kidney histology similar to wild-type controls. However, CBAxB6-TGFβ mice manifested glomerular hypertrophy with mesangial expansion and capillary obliteration affecting 60% of glomeruli, together with mild tubulointerstitial fibrosis and tubular hyaline deposits (Figure 1d–f [right panel of f]). Significant glomerular and tubulointerstitial collagen-4 (Figure 2a and b) and

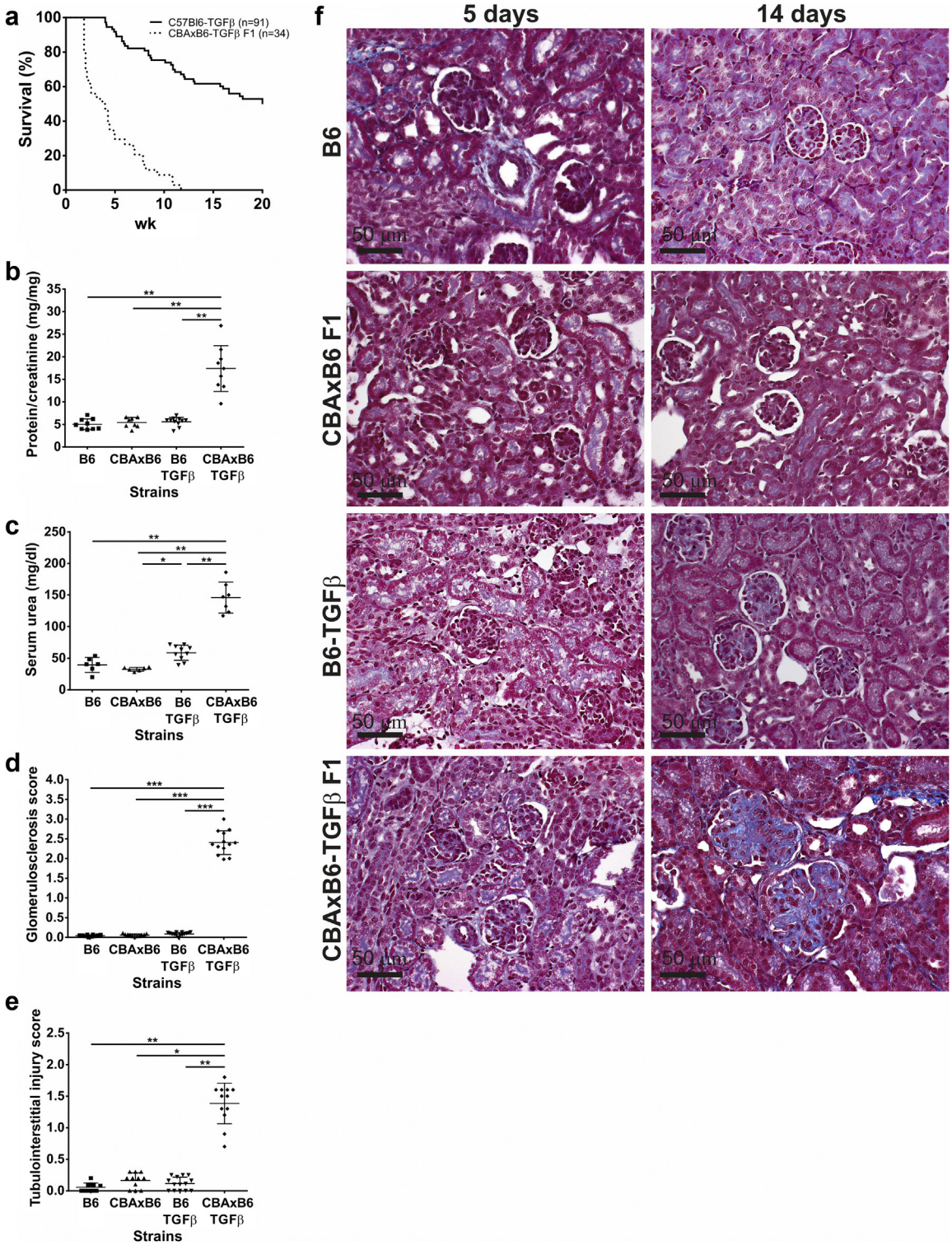

Figure 1 | Characterization of transforming growth factor-beta1 (TGF-β_1) transgenic mice and controls. (**a**) Survival time of (dotted line) CBAxB6-TGFβ mice ($n = 34$) was dramatically shorter, compared with that of (solid line) B6-TGFβ mice ($n = 91$; Kaplan-Meier analysis, $P < 0.0001$). (**b**) Urine protein-to-creatinine ratio ($n = 8$–11/group) and (**c**) serum urea levels ($n = 6$–10/group) were only elevated in CBAxB6-TGFβ F1 mice. Histology scores ($n = 10$–14/group) for (**d**) glomerulosclerosis and (**e**) tubulointerstitial damage show significant fibrosis with mesangial expansion in CBAxB6-TGFβ F1 mice, compared with B6-TGFβ and wild-type mice. (**f**) The histopathology is shown on representative photomicrographs of paraffin-embedded kidney sections comparing TGF-β_1 transgenic and wild-type control mice at ages 5 days (left panel) and 14 days (right panel). B6-TGFβ kidneys had no histologic alterations in any time points, compared with wild-type controls. CBAxB6-TGFβ F1 kidneys showed mild enlargement and sclerosis in some glomeruli at age 5 days, but severe glomerular hypertrophy and sclerosis at age 14 days (Masson's trichrome stain; original magnification ×400; bar = 50 μm). Data are presented as mean ± SD. Kruskal-Wallis test, $^*P < 0.05$; $^{**}P < 0.01$; $^{***}P < 0.001$. To optimize viewing of this image, please see the online version of this article at www.kidney-international.org.

Table 1 | Pathology and laboratory data of transgenic B6-TGFβ and CBAxB6-TGFβ F1 mice and wild-type controls, at age 14 days

Mouse strain	Body weight, g	Kidney weight/body weight, mg/g	Plasma TGF-β_1, ng/ml	Urea nitrogen, mg/dl	Proteinuria, mg protein/mg creatinine
B6 ($n = 10$)	7.25 ± 0.62	7.60 ± 1.03	4.04 ± 2.01	36.5 ± 10.6	5.03 ± 1.18
CBAxB6 F1 ($n = 8$)	8.45 ± 0.95[a]	7.40 ± 0.79	3.10 ± 1.76	34.8 ± 6.4	5.41 ± 1.11
B6-TGFβ ($n = 14$)	7.21 ± 0.87[c]	7.14 ± 0.55	57.61 ± 16.77[a,c]	58.5 ± 11.9[a,c]	5.58 ± 0.97
CBAxB6-TGFβ F1 ($n = 15$)	8.54 ± 1.06[a,b]	9.94 ± 1.03[a,b,c]	44.49 ± 19.15[a,c]	152.0 ± 31.8[a,b,c]	15.20 ± 6.66[a,b,c]
ANOVA/Kruskal-Wallis	$P < 0.0001$	$P < 0.0001$	$P < 0.0001$	$P < 0.0001$	$P < 0.005$

ANOVA, analysis of variance; TGFβ, transforming growth factor-beta.
[a]$P < 0.05$ vs. B6.
[b]$P < 0.05$ vs. B6-TGFβ.
[c]$P < 0.05$ vs. CBAxB6 F1.
Data from male TGF-β1 transgenic mice and male wild-type controls at the age of 14 days are shown. Despite having plasma TGFβ$_1$ levels similar to those of B6-TGFβ mice, CBAxB6-TGFβ mice had significant renal hypertrophy, accompanied by elevated serum urea nitrogen levels and proteinuria. Values are expressed as mean ± SD. ANOVA or Kruskal-Wallis test.

fibronectin accumulation were present (Figure 2c and d). Glomerular expression of TGFB1 protein was significant in only CBAxB6-TGFβ kidneys (Figure 2e and f), whereas mild tubular expression was present in B6-TGFβ as well.

The evaluation of renal cortical gene expression at age 14 days showed that collagen-1 (*Cola1*) and collagen-3 (*Col3a1*) mRNA expression in B6-TGFβ kidneys were mildly elevated, compared with that in controls, and were significantly increased (5- and 4-fold, respectively) in kidneys of CBAxB6-TGFβ mice (Figure 3a and b). This increase was accompanied by renal *Lcn2* (Figure 3c), *Tgfb1*, and connective tissue growth factor (*Ctgf*) mRNA overexpression in CBAxB6-TGFβ mice (Table 2), in parallel with increased expression of the TGF-β1 inhibitors biglycan (*Bgn*) and decorin (*Dcn*; Table 2). At the age of 14 days, expression of matrix metalloproteinase-2 (*Mmp2*) was similar in wild-type and transgenic kidneys. No significant alteration occurred in the expression of TGF-β_1 receptor-II (*Tgfbr2*) or any of the Smad mRNAs (*Smad2*, *3*, *4*, *6*, *7*) or SMAD3 phosphorylation (Supplementary Figure S2A). Interestingly, *Mmp9* levels in B6 and B6-TGF-β kidneys were comparable, whereas CBAxB6 and CBAxB6-TGF-β kidneys had 3- to 4-fold increases in *Mmp9* mRNA expression, respectively. Expression of *Timp2* mRNA was comparable in wild-type and B6-TGFβ kidneys, but it was elevated in CBAxB6-TGF-β mice (Table 2).

Strikingly, a 100-fold increase occurred in *Timp1* mRNA expression in CBAxB6-TGFβ kidneys, compared to that in B6-TGF-β and wild-type mice (Figure 3d). Immunoblot analysis revealed a 10-fold increase in TIMP1 protein expression (Figure 3e), mainly localized to tubules in CBAxB6-TGFβ kidneys (Figure 3g). This TIMP1 overexpression in CBAxB6-TGFβ kidneys resulted in reduced renal matrix metalloproteinase-9 (MMP9) activity, as shown by gelatin zymography (Figure 3f).

We wished to elucidate whether either the hepatic expression of the TGF-β transgene exerts local fibrotic effects in the liver or the elevated plasma TGF-β_1 levels distantly affect the heart in ways that could substantially contribute to the short survival time of CBAxB6-TGFβ mice. However, the extent of fibrosis in the liver and the myocardial expression of *Col1a1* mRNA were similar in the 2 transgenic strains (Supplementary Figure S2B and C).

To investigate whether alterations in other kidney disease–related genes could be responsible for this phenotype, we performed cDNA microarray analysis of B6-TGFβ and CBAxB6-TGFβ kidneys. The microarray showed 311 significant gene alterations (Supplementary Figures S3 and S4; Supplementary Tables S4 and S5) and confirmed that *Timp1* is the most upregulated gene related to matrix remodeling. Significant changes in RNA expression were seen for 27 transcription factors (Supplementary Table S6). Among them, *Egr2* was the most strikingly induced in CBAxB6-TGFβ kidneys (Figure 4a–c). EGR2 drew our attention, as it has been implicated in the pathogenesis of skin and lung fibrosis.[16] Of note, renal expression of *Egr2* mRNA was similar in B6-TGFβ and wild-type mice (Figure 4a–c). We observed nuclear EGR2 protein expression mostly in some interstitial cells in control kidneys and B6-TGFβ mice; this increased significantly in CBAxB6-TGFβ kidneys, accompanied by tubular overproduction that coexpressed with TIMP1 (Figure 4c).

EGR2 and TIMP-1 overexpression are hallmarks of fibrosis initiation in TGFβ-transgenic mice

As histology revealed nearly end-stage glomerulosclerosis in CBAxB6-TGFβ (F1) kidneys at age 14 days, we investigated the initiation and early development of kidney fibrosis in TGF-β1–transgenic mice at birth and at 5 days. Glomerular size and mesangial matrix content increased significantly in CBAxB6-TGFβ mice at 5 days (glomerulosclerosis index [GSI] B6-TGFβ: 0.05 ± 0.01 vs. CBAxB6-TGFβ: 0.45 ± 0.21, $P < 0.05$; Figure 1f, left). Renal *Tgfb1* mRNA expression in 5-day-old CBAxB6-TGFβ mice was also significantly higher compared to that in B6-TGF-β or controls (Table 3), although expression of *Ctgf*, and type-I (*Col1a1*) and type III (*Col3a1*) collagens, was similar in all groups at this age. However, *Timp1* mRNA expression at this early age was 50% higher in CBAxB6-TGFβ kidneys, accompanied by elevated *Egr2* expression (Table 3). In B6-TGFβ kidneys, EGR2 immunostaining was observed in interstitial cells, similar to that in

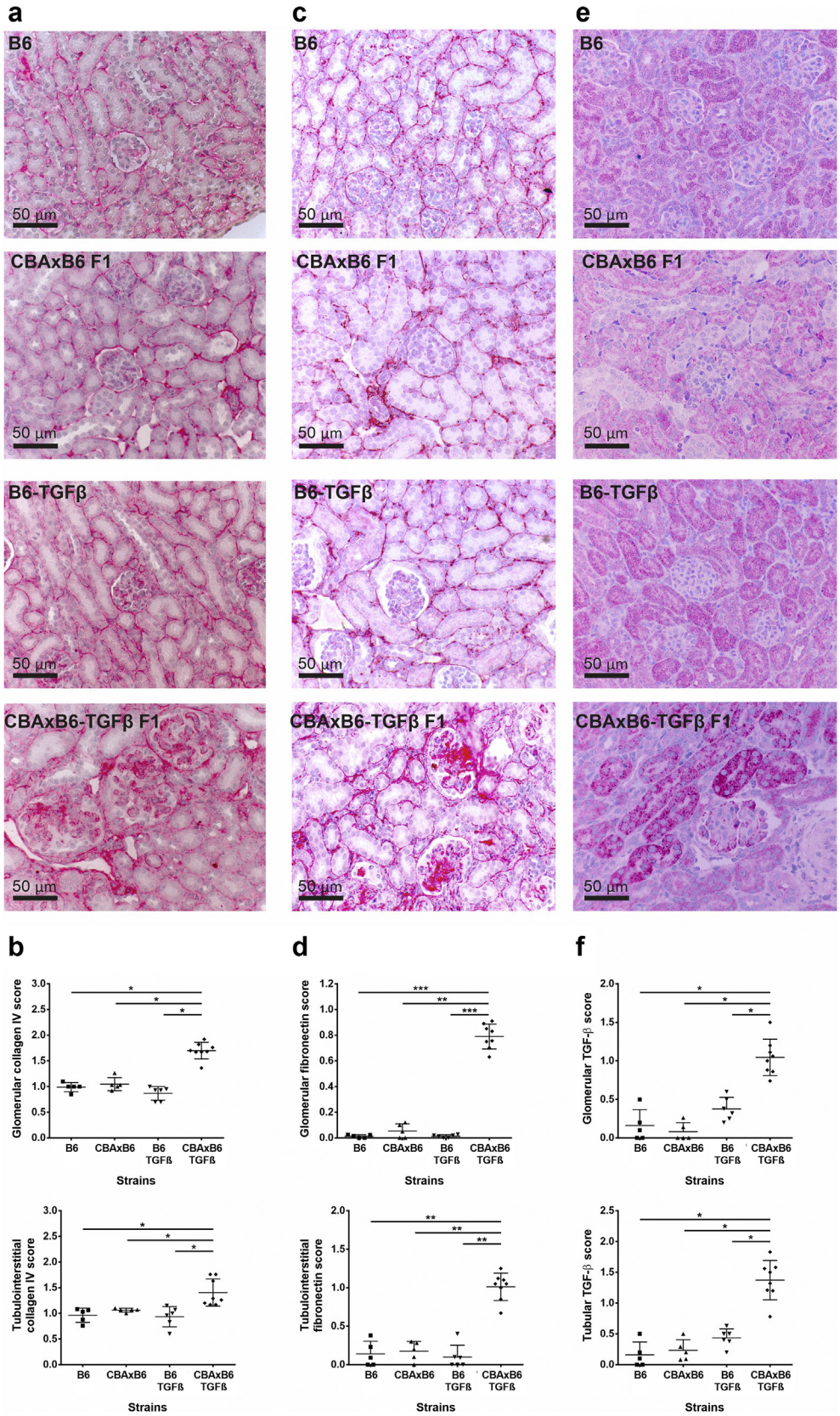

Figure 2 | Renal expression of transforming growth factor-beta (TGF-β) and extracellular matrix proteins. Evaluation of renal type-IV collagen, fibronectin, and TGF-β_1 immunostaining in TGF-β transgenic mice and wild-type controls at age 14 days. (**a**) Representative photomicrographs of type IV collagen expression depict a marked increase in CBAxB6-TGFβ kidneys, (**b**) both in glomeruli and tubulointerstitium. The similar patterns in (**c,d**) renal fibronectin and (**e,f**) TGF-β_1 immunostaining scores further underscore the marked fibrosis in CBAxB6-TGFβ (continued)

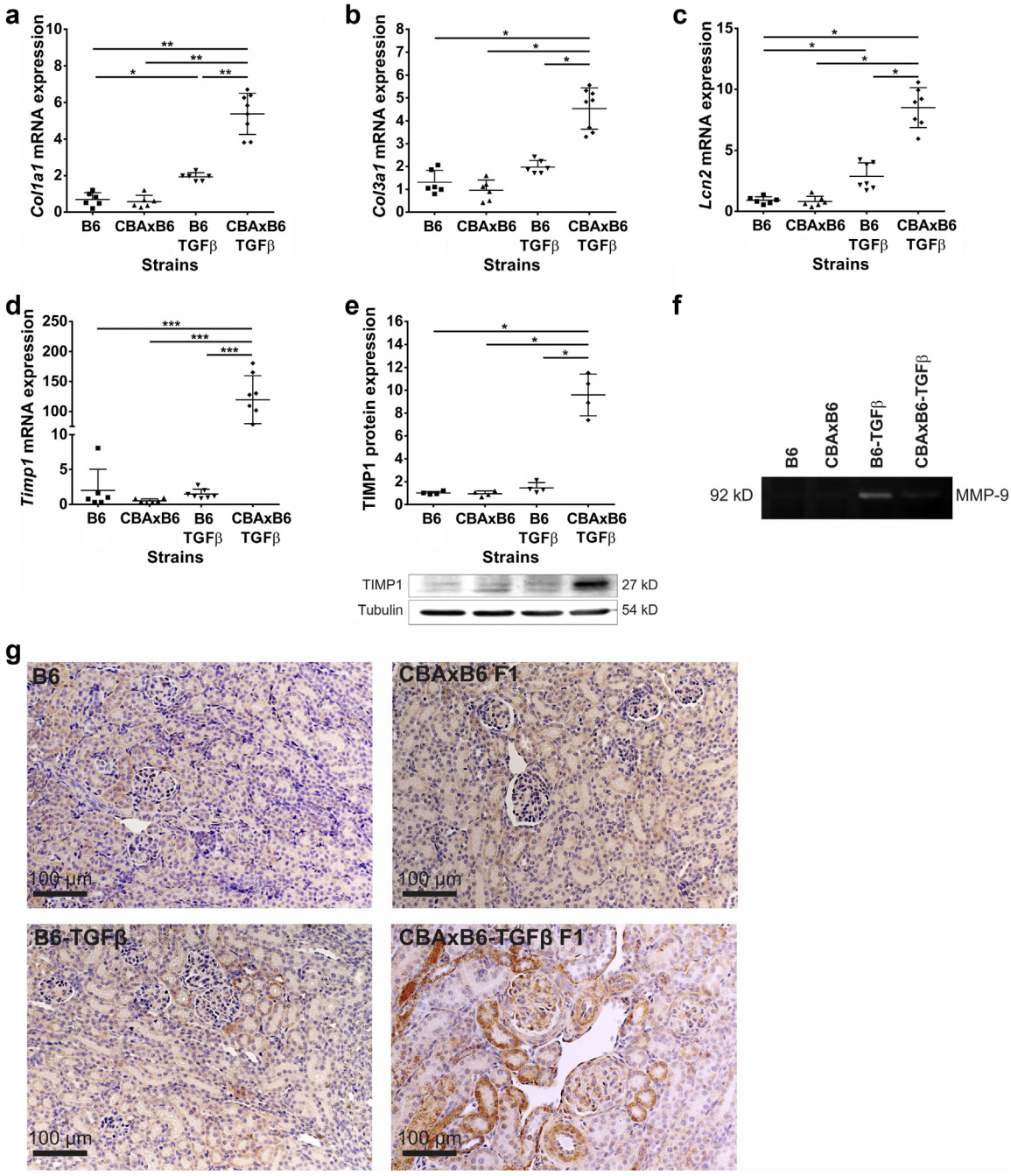

Figure 3 | Renal expression of mRNA encoding extracellular matrix and related proteins. Renal cortical expression of (**a**) type I collagen and (**b**) type III collagen, (**c**) lipocalin-2 (*Lcn2*), and (**d**) tissue inhibitor of matrix metalloproteinase-1 (TIMP-1) mRNA in wild-type and transforming growth factor-beta1 (TGF-β_1) transgenic mouse strains at age 14 days (n = 6–8/group). (**e**) TIMP1 immunoblot analysis (n = 4/group) shows a 10-fold increase in CBAxB6-TGFβ kidneys, which was shown to be mainly localized to (**g**) tubules by immunostaining (original magnification ×200; bar = 100 µm) and (**f**) resulted in reduced renal matrix metalloproteinase-9 (MMP9) gelatinase activity, as shown by representative zymography. All data are presented as fold expression to control sample (mean ± SD). Kruskal-Wallis test, $^*P < 0.05$; $^{**}P < 0.01$; $^{***}P < 0.001$. To optimize viewing of this image, please see the online version of this article at www.kidney-international.org.

controls, despite a mild tubular TIMP1 immunostaining (Supplementary Figure S5). However, EGR2 and TIMP1 were already coexpressed in tubules of CBAxB6-TGFβ mice at this early age, although to a lesser extent than in 14-day-old mice (Figure 4c). In contrast, kidneys of newborn B6-TGFβ and CBAxB6-TGFβ mice depicted no renal histologic alterations

Figure 2 | (continued) kidneys. (**a,c,e**) Original magnification ×400; bar = 50 µm. Data are presented as mean ± SD (n = 6–8/group). Kruskal-Wallis test, $^*P < 0.05$; $^{**}P < 0.01$; $^{***}P < 0.001$. To optimize viewing of this image, please see the online version of this article at www.kidney-international.org.

Table 2 | Renal expression of fibrosis pathway genes in transgenic B6-TGFβ and CBAxB6-TGFβ F1 mice at age 14 days

Gene symbol	B6 (n = 5)	CBAxB6 F1 (n = 5)	B6-TGFβ (n = 7)	CBAxB6-TGFβ F1 (n = 7)	Kruskal-Wallis test
Tgfb1	1.00 ± 0.18	1.05 ± 0.12	0.80 ± 0.17	1.61 ± 0.42[a,b,c]	$P < 0.0001$
Ctgf	1.00 ± 0.19	0.69 ± 0.13	0.29 ± 0.06	1.88 ± 0.56[a,b,c]	$P < 0.0001$
Bgn (biglycan)	1.00 ± 0.39	0.37 ± 0.06	1.01 ± 0.23	1.78 ± 0.46[a,b,c]	$P < 0.0001$
Dcn (decorin)	1.00 ± 0.28	0.43 ± 0.13	1.09 ± 0.27[c]	1.84 ± 0.43[a,b,c]	$P < 0.0001$
Mmp2	1.00 ± 0.29	0.40 ± 0.21	0.97 ± 0.19	0.91 ± 0.38	NS
Mmp9	1.00 ± 0.33	3.24 ± 0.57[a]	0.88 ± 0.30[c]	4.06 ± 1.04[a,b]	$P < 0.0001$
Timp1	1.00 ± 0.53	0.52 ± 0.28	1.39 ± 0.45	108.48 ± 28.57[a,b,c]	$P < 0.0001$
Timp2	1.00 ± 0.20	0.61 ± 0.08	0.98 ± 0.09	1.53 ± 0.11[c]	$P < 0.05$
Timp3	1.00 ± 0.21	1.31 ± 0.24	1.16 ± 0.07	1.35 ± 0.39	NS
Tgbr2	1.00 ± 0.13	0.91 ± 0.15	1.03 ± 0.34	1.15 ± 0.16	NS
Smad2	1.00 ± 0.34	0.72 ± 0.18	0.86 ± 0.14	0.95 ± 0.39	NS
Smad3	1.00 ± 0.08	0.81 ± 0.19	0.89 ± 0.12	1.03 ± 0.23	NS
Smad4	1.00 ± 0.28	0.85 ± 0.22	0.97 ± 0.12	0.91 ± 0.24	NS
Smad6	1.00 ± 0.47	0.95 ± 0.39	1.12 ± 0.19	1.10 ± 0.60	NS
Smad7	1.00 ± 0.10	0.70 ± 0.17	0.86 ± 0.11	1.07 ± 0.24	NS

TGFβ, transforming growth factor-beta; NS, not significant.
[a]$P < 0.05$ vs. B6.
[b]$P < 0.05$ vs. B6-TGFβ.
[c]$P < 0.05$ vs. CBAxB6 F1.
Renal mRNA expression values of male TGF-β1 transgenic mice and male wild-type controls at age 14 days. Expression of each gene was normalized to 18S rRNA (*Rn18s*) using the $2^{-\Delta\Delta Ct}$ formula. Data are presented as fold expression to a pooled control sample (mean ± SD).

(data not shown) and had comparable *Timp1* and *Egr2* mRNA expression levels. The kinetics of *Egr2* and *Timp1* mRNA expression from 0 to 14 days of age, while only correlative, could indicate a mechanistic role for EGR2 and TIMP1 in the pathophysiological process of kidney fibrosis in this model (Figure 4d and e).

TIMP-1 neutralization reduced fibrosis in CBAxB6-TGFβ F1 transgenic mice

As these data suggested the central role of TIMP1 in TGF-β1–induced kidney fibrosis, we injected male CBAxB6-TGFβ mice i.p. with anti-TIMP1 neutralizing antibody or isotype IgG for 5 consecutive days, beginning at age 8 days, and the animals were euthanized at age 14 days. The early systemic TIMP1 inhibition was associated with a 20% reduction in kidney weight in fibrosis-prone CBAxB6-TGFβ mice, compared to that in isotype IgG-treated transgenic littermates (Figure 5a), accompanied by a 50% reduction in proteinuria (Figure 5b) and serum urea levels (Figure 5c), and by less glomerular and tubulointerstitial damage than in IgG-treated littermates (Figure 5d–f).

Early EGR2 and TIMP1 overexpression is associated with progression after UUO and SNX

In order to test whether strain-dependent early onset kidney fibrosis is associated with EGR2 or TIMP1 protein overexpression in other fibrosis models, we investigated B6 and CBA wild-type mice after UUO and SNX. Overt kidney fibrosis usually develops 3–5 days after UUO.[17] We first examined young wild-type B6 and CBA male mouse kidneys 24 hours after UUO. Kidney histology at this early stage showed only a few dilated tubules, otherwise normal structure, and no signs of extracellular matrix accumulation (Figure 6a). Renal mRNA expression of *Lcn2*, as a marker of tubular damage (Figure 6b) and *Tgfb1* (Figure 6c), increased comparably in both B6 and CBA UUO. By contrast, *Col1a1* mRNA expression was 2-fold higher in CBA UUO, compared with that in B6 UUO kidneys (Figure 6d), and was accompanied by significant overexpression of *Egr2* and *Timp1* mRNA (Figure 6e and f) and EGR2 protein (Supplementary Figure S6A and B). The higher TIMP1 expression resulted in lower renal MMP9 activity in CBA UUO kidneys (Figure 6g and h). We also analyzed kidneys at 7 days after UUO, at which point significant interstitial fibrosis had developed in B6, but slightly more-severe fibrosis had developed in CBA kidneys, accompanied by higher *Timp1* mRNA expression and reduced renal MMP9 activity, but only *Egr2* mRNA expression tended to be higher in CBA at this late time point (Supplementary Figure S7A–D).

In the second set of experiments, we observed marked interstitial fibrosis and glomerulosclerosis in male CBA mice at 6 weeks after SNX, compared with B6 mice (Figure 7a and b). The significant renal fibrosis of CBA SNX mice was associated with an elevated urinary protein-to-creatinine ratio (Figure 7c), although *Tgfb1* mRNA was comparable in B6 and CBA SNX mice (Figure 7d). However, CBA SNX kidneys overexpressed *Col1a1* and *Lcn2* mRNA (Figure 7e and f), as well as TIMP1 (Figure 7g and h), EGR2 mRNA, and protein (Figure 7i; Supplementary Figure S8), the latter of which co-localized with TIMP1, as shown by immunostaining in most of the CBA SNX tubules (Figure 7h).

TIMP1 deficiency inhibits the development of fibrosis after SNX in CBAxB6 mice

In order to confirm the central role of TIMP1 in the initiation and progression of kidney fibrosis, we compared TIMP1-deficient (Timp1-null) male mice on a fibrosis-prone CBAxB6 background, to wild-type CBAxB6 F1 male mice (Timp1+) subjected to SNX. Six weeks after nephrectomy, Timp1+ SNX kidneys manifested

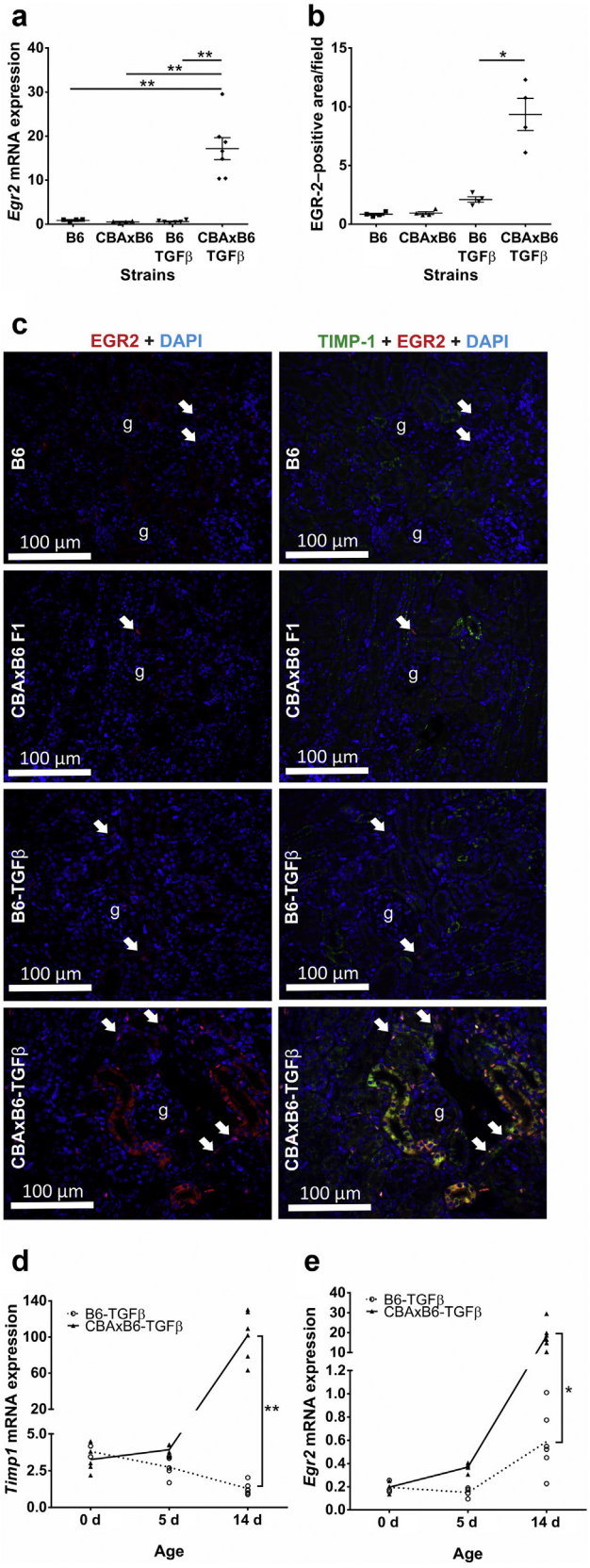

Figure 4 | Renal early growth response factor-2 (EGR2) expression in wild-type and transforming growth factor-beta1 (TGF-β_1) transgenic mouse strains. At 14 days of age, EGR2 increased markedly in only CBAxB6-TGFβ kidneys, at (continued)

glomerulosclerosis, tubular atrophy, and interstitial matrix accumulation, whereas Timp1-null SNX kidneys exhibited only mild, nonsignificant glomerulosclerosis and interstitial fibrosis (Figure 8a and b). This difference was reflected by a marked difference in proteinuria (Figure 8c). Of note, expression of type I and type III collagen mRNA was slightly but significantly elevated in Timp1-null SNX kidneys (Figure 8d and e), even though their histology was similar to that of control kidneys. Notably, Timp1+ SNX kidneys had 10-fold increased expression of *Col1a1* and *Col3a1*, accompanied by a 2-fold increase in *Tgfb1* mRNA (Figure 8f). In contrast, Timp1-null SNX kidneys had *Tgfb1* expression similar to that in controls. The lack of TIMP1 resulted in higher MMP9 gelatinase activity in Timp1-null SNX kidneys (Figure 8g).

In vitro overexpression of EGR2 upregulates TIMP1, whereas EGR2 silencing reduces TIMP1

For *in vitro* evaluation of a possible EGR2-TIMP1 regulation, we transiently transfected human embryonic kidney (HEK)293 cells with mammalian expression vector plasmid containing cytomegalovirus (CMV) promoter and full-length *Egr2* gene (pEGR2). Controls either were transfected with EGFP coding plasmid (pEGFP) or received only the transfection reagent Lipofectamine 3000 (Lipo). Transfection with pEGR2 for 24 hours significantly increased EGR2 protein expression, which plausibly was responsible for overexpression of TIMP-1 mRNA and protein, by 2.5-fold and 4-fold, respectively (Figure 9a and b). Further, EGR2 levels correlated with TIMP-1 (Figure 9c). In another set of experiments, we transfected human kidney (HK)–2 cells with *EGR2* small, interfering (si)RNA or scrambled siRNA 24 hours prior to TGF-β treatment. Silencing *EGR2* inhibited TGF-β–induced EGR2 and TIMP1 production and increased the MMP9 gelatinase activity of HK-2 cells (Figure 9d and e). Interestingly, TGF-β induced *TIMP1* and *EGR2* mRNA overexpression in human fibroblasts also (Supplementary Figure S9). *In vivo*, EGR2 siRNA administration prior to UUO significantly lowered renal EGR2,

Figure 4 | (continued) both the (**a**) mRNA and (**b**) protein levels. (**c**) Representative photomicrographs of immunostaining show (red) EGR2 mostly in the (see arrows) tubulointerstitium of control and B6-TGFβ kidneys with (green) minimal tubular tissue inhibitor of matrix metalloproteinase-1 (TIMP1) positivity. Apart from its interstitial increase and to a lesser extent, glomerular staining, EGR2 also appeared in tubules of CBAxB6-TGFβ mice, where it mostly co-localized with TIMP1 (yellow; original magnification ×400; bar = 50 μm). The kinetics of both (**d**) *Timp1* and (**e**) *Egr2* in kidneys of B6-TGFβ and CBAxB6-TGFβ F1 transgenic mice at the age of 0 days (n = 3/group), 5 days (n = 5/group), and 14 days (n = 6/group) show early overexpression only in CBAxB6-TGFβ F1 mice. Data are presented as fold expression to control sample (mean ± SD; n = 4–7/group). Kruskal-Wallis test, *$P < 0.05$; **$P < 0.01$. DAPI, 4′,6-diamidino-2-phenylindole; g, glomerulus. To optimize viewing of this image, please see the online version of this article at www.kidney-international.org.

Table 3 | Renal expression of fibrosis-related genes in transgenic B6-TGFβ and CBAxB6-TGFβ F1 mice at age 5 days

Gene symbol	B6 (n = 4)	CBAxB6 F1 (n = 4)	B6-TGFβ (n = 6)	CBAxB6-TGFβ F1 (n = 6)	Kruskal-Wallis test
Tgfb1	1.00 ± 0.25	1.09 ± 0.06	0.83 ± 0.15	1.34 ± 0.32[a,b,c]	$P < 0.05$
Ctgf	1.00 ± 0.06	1.14 ± 0.23	1.01 ± 0.32	1.18 ± 0.07	NS
Col1a	1.00 ± 0.36	0.85 ± 0.14	1.08 ± 0.30	1.01 ± 0.37	NS
Col3a1	1.00 ± 0.25	0.78 ± 0.14	1.07 ± 0.45	1.13 ± 0.29	NS
Mmp2	1.00 ± 0.11	0.89 ± 0.14	0.90 ± 0.10	1.75 ± 0.90[a,b,c]	$P < 0.05$
Mmp9	1.00 ± 0.35	0.92 ± 0.21	1.06 ± 0.69	1.27 ± 0.51	NS
Timp1	1.00 ± 0.53	1.25 ± 0.50	1.02 ± 0.44	1.94 ± 0.62[a,b,c]	$P < 0.05$
Egr2	1.00 ± 0.26	0.94 ± 0.31	0.99 ± 0.27	2.20 ± 0.42[a,b,c]	$P < 0.001$

TGFβ, transforming growth factor-beta; NS, not significant.
[a]$P < 0.05$ vs. B6.
[b]$P < 0.05$ vs. B6-TGFβ.
[c]$P < 0.05$ vs. CBAxB6 F1.
Timp1 and *Egr2* expression were already elevated in CBAxB6-TGFβ mice at this very early age. Gene expression was normalized to 18S rRNA (*Rn18s*) using the $2^{-\Delta\Delta Ct}$ formula. Data are presented as fold expression to a pooled control sample (mean ± SD).

accompanied by reduced TIMP1 expression (Supplementary Figure S10A and B).

Increased EGR2 and TIMP1 expression in human FSGS kidney biopsies

In order to test whether upregulation of EGR2 and TIMP-1 in mice, and the coregulation in HEK293 and HK-2 cells, has human clinical relevance, we investigated human kidney cortex biopsies obtained from FSGS patients and controls (the latter samples were taken from healthy cortex area of kidneys removed due to renal cancer (Supplementary Table S7). We observed more than 2-fold overexpression of both *EGR2* and *TIMP1* mRNA in FSGS samples, compared with that in control tissues (Figure 9f), despite nonsignificant differences in *TGFB1* mRNA. Immunostaining revealed increased tubular EGR2 and TIMP1 expression in FSGS biopsies, with notable coexpression in several tubules (Figure 9g).

DISCUSSION

Experimental animal and human studies have demonstrated that TGF-β1 plays a central role in the initiation and progression of kidney fibrosis. CBA.B6-Alb/TGF-β1 transgenic mice maintained on mixed (CBAxB6) genetic background developed kidney fibrosis characterized as either mild or severe,[15] presumably as a consequence of the inhomogeneous genetic background. In the present study, we generated congenic B6-TGFβ transgenic mice manifesting only a mild renal phenotype, and CBAxB6-TGFβ F1 mice that exhibited shortened survival time, proteinuria, and glomerulosclerosis. We identified the transcription factor EGR2 (Krox-20) as a novel participant in the development of progressive renal fibrosis in mice and FSGS patients. We also demonstrate that the genetic background of mice (B6 vs. CBA) is strongly associated with an altered early EGR2 and downstream TIMP-1 response, which contributes to the progression of fibrosis in various models, including UUO, SNX, and TGF-β1–transgenic mice.

We have addressed the hypothesis that genetic differences among inbred mouse strains contribute to the variability in TGF-β1–induced progressive fibrosis, and we sought evidence for specific differences in expression of relevant molecules. Although the backcross of TGF-β1 transgene mice to the inbred B6 strain (congenic B6-TGFβ mice) did not reduce the elevated plasma TGF-β1 levels, B6-TGFβ mice developed only mild glomerulosclerosis, lacked proteinuria, and had significantly improved survival (Figure 1). Our finding corroborates reports of B6 mice as a strain that is resistant to renal fibrosis.[10,12,13]

We also wished to examine the effects of CBA genetic background on progression of kidney fibrosis. The CBAxB6-TGFβ transgenic mice had elevated plasma TGF-β1 levels, similar to those of the B6-TGFβ strain, although their renal disease was markedly accelerated and their survival time was greatly shortened, compared with those of B6-TGFβ mice. CBAxB6-TGFβ mice manifested glomerular matrix accumulation as soon as 5 days of age (Figure 1f), and 50% of these mice succumbed to uremic death by age 21 days. Our study provides evidence that genetic background strongly influences the profibrotic effect of TGF-β1 in this model. We observed similar genetic differences in the progression of kidney disease using 2 classical models of renal fibrosis, the UUO model (Figure 6) and the SNX (Figure 7).

The analysis of fibrosis-related molecules in CBAxB6-TGFβ mouse kidneys revealed several-fold increases in mRNA expression of *Tgfb1* and interstitial collagens at as early as 14 days of age, compared to that in B6-TGFβ mice. The observed strain differences were not related to altered expression of the natural inhibitors of TGF-β_1[18,19] or to TGF-β_1 signaling molecules.[20]

TGF-β1 influences the extracellular matrix turnover by repressing matrix metalloproteinases (MMPs) and inducing their tissue inhibitors (TIMPs).[21] MMP2 cleaves fibronectin and collagen-1 and -3,[22] whereas MMP9 cleaves collagen-4 with higher affinity.[23] Among their inhibitors, TIMP-1, -2, and -3 are expressed in the kidney.[23] Analysis of TIMPs in TGFβ1-transgenic mice revealed a striking TIMP-1 overexpression in CBAxB6-TGFβ kidneys, compared to that in B6-TGFβ mice, mainly localized in tubules, that resulted in reduced MMP9 gelatinase activity. Additionally, the transcription factor EGR2 was

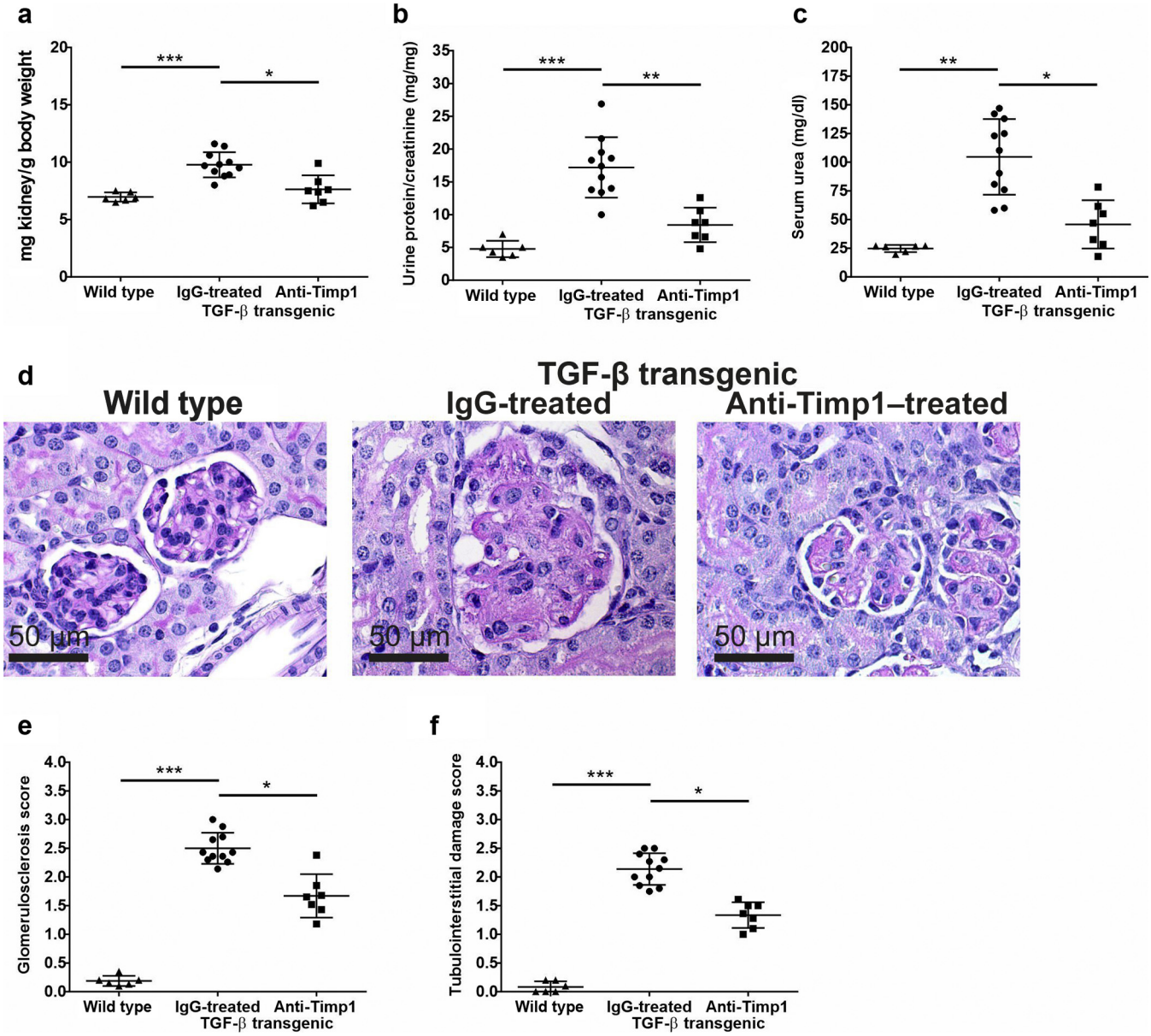

Figure 5 | Effects of tissue inhibitor of matrix metalloproteinase-1 (TIMP-1) neutralization in fibrotic CBAxB6-transforming growth factor-beta (TGFβ) mice. TIMP-1 neutralization for 5 consecutive days significantly reduced (**a**) renal hypertrophy, (**b**) proteinuria, and (**c**) serum urea levels in CBAxB6-TGFβ F1 mice. Administration of anti–TIMP-1 antibody ameliorated (**d,e**) glomerulosclerosis and (**d,f**) tubulointerstitial fibrosis, as compared to isotype IgG-treated CBAxB6-TGFβ F1 mice. Periodic acid–Schiff staining, original magnification ×400. Data are presented as mean ± SD for CBAxB6 F1 (wild-type, $n = 5$), IgG-treated CBAxB6-TGFβ F1 (IgG-treated TGF-β transgenic, $n = 12$) and anti–TIMP-1–treated CBAxB6-TGFβ F1 mice (anti-Timp1 TGF-β transgenic, $n = 7$). *$P < 0.05$, **$P < 0.01$, ***$P < 0.001$ (Kruskal-Wallis test and analysis of variance). To optimize viewing of this image, please see the online version of this article at www.kidney-international.org.

significantly induced and correlated to TIMP-1 in CBAxB6-TGFβ kidneys. EGR2 has been described as a key mediator of TGF-β action in mouse models of scleroderma and lung fibrosis, and in human scleroderma.[16] Of note, Vollmann and colleagues found that *in vivo EGR2* gene silencing reduces liver fibrosis in mice.[24] To the best of our knowledge, the present study is the first to link EGR2 to renal fibrosis progression. As several pathways (including inflammation) were upregulated in the microarray study, we might also consider them as possible contributors to the pathogenesis. We focused on EGR2 as the most upregulated transcription factor, and TIMP-1 as the most overexpressed participant of extracellular matrix remodeling. The importance of TIMP-1 in kidney fibrosis has been postulated, as elevated TIMP-1 levels have been reported in human diabetic nephropathy[25] and glomerulonephritis,[26] and in experimental models of murine lupus glomerulonephritis,[27] protein overload proteinuria,[28] and

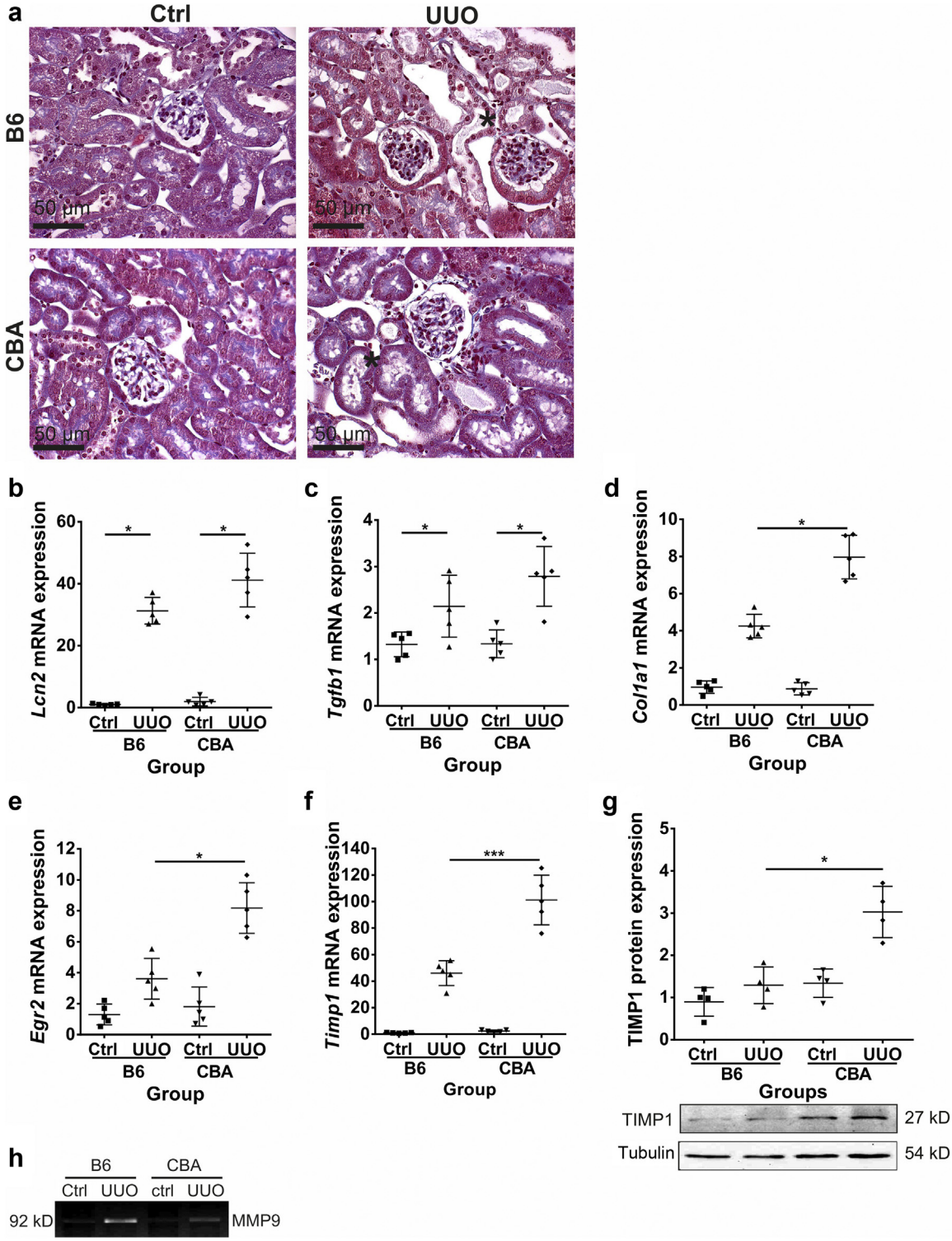

Figure 6 | Strain-related early differences in *Egr2* and *Timp1* after unilateral ureter obstruction (UUO). After UUO in both B6 and CBA mice, we observed (**a**) a similar extent of tubular dilation within 24 hours (asterisks show dilated tubules). (**b**) Renal mRNA expression of lipocalin-2 *(Lcn2)* and (**c**) transforming growth factor-beta (TGF-β) (*Tgfb1*) were similarly elevated in both B6 and CBA UUO mice. However, (**d**) renal type-I collagen (*Col1a1*), (**e**) *Egr2*, and (**f**) *Timp1* mRNA expressions ($n = 5$/group) were significantly higher in CBA UUO, compared with that in B6 UUO kidneys, accompanied by an already 2-fold tissue inhibitor of matrix metalloproteinase-1 (TIMP1) protein overexpression ($n = 4$/group) in (**g**) CBA UUO at this early stage. (**h**) The increased TIMP1 reduced matrix metalloproteinase-9 (MMP9) activity in CBA UUO, compared with that in B6 UUO, as shown by representative gelatin zymography. All data are presented as fold expression to control (Ctrl) sample (mean ± SD). Kruskal-Wallis test, $^{*}P < 0.05$; $^{***}P < 0.001$. To optimize viewing of this image, please see the online version of this article at www.kidney-international.org.

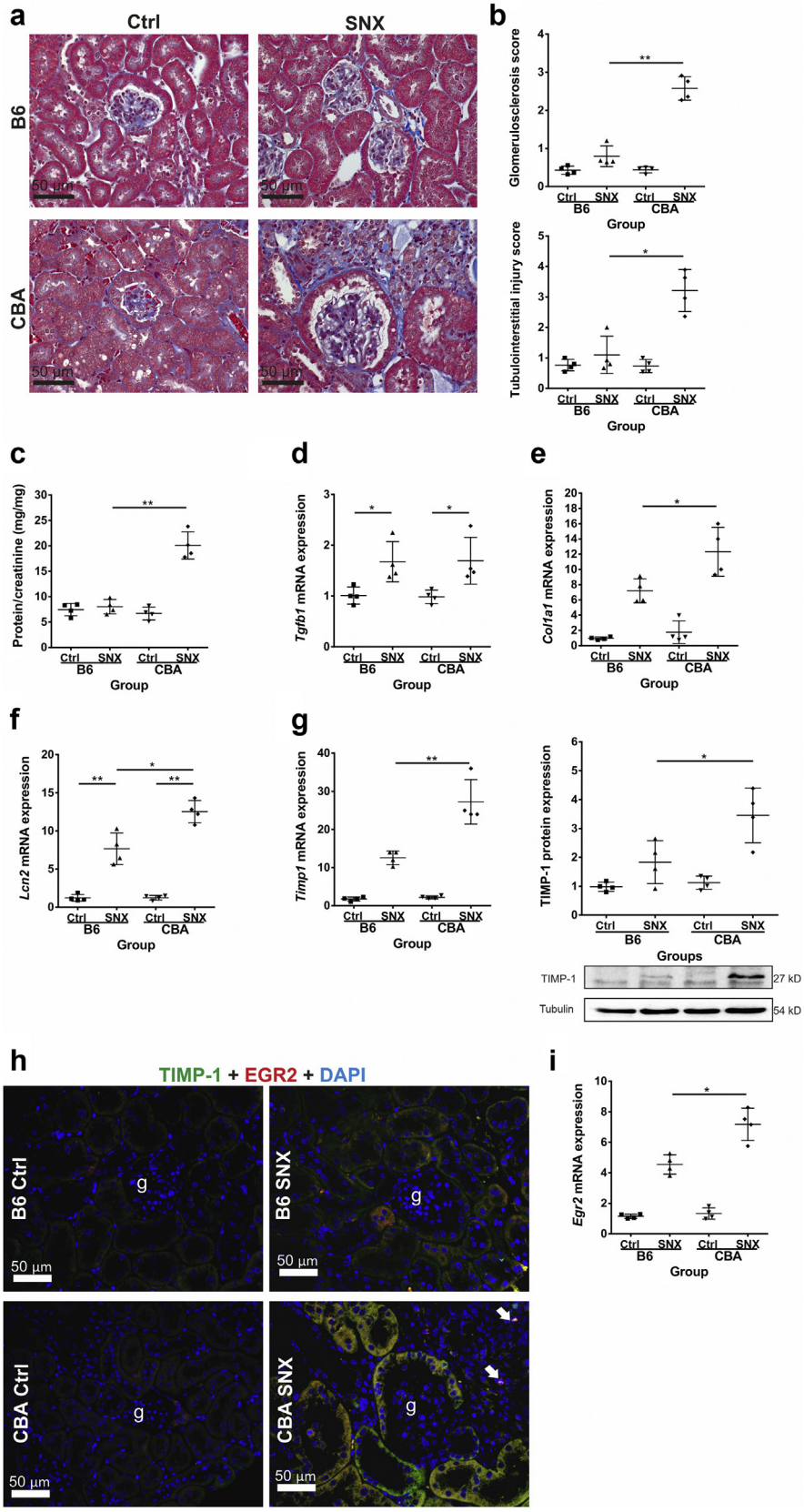

Figure 7 | Strain-related differences in *Egr2* and *Timp1* after subtotal renal ablation (SNX). Six weeks after SNX, we observed (**a,b**) only mild glomerular scarring and tubulointerstitial fibrosis in B6 mice, but severe glomerulosclerosis and interstitial fibrosis in CBA mice. (**c**) CBA SNX mice developed marked proteinuria despite the fact that the (**d**) transforming growth factor-beta (TGF-β) mRNA (*Tgfb1*) expression was comparable to that in B6 SNX. (**e**) Kidneys of CBA SNX mice showed overexpression of type-I collagen mRNA (*Col1a1*) and (**f**) lipocalin-2 (continued)

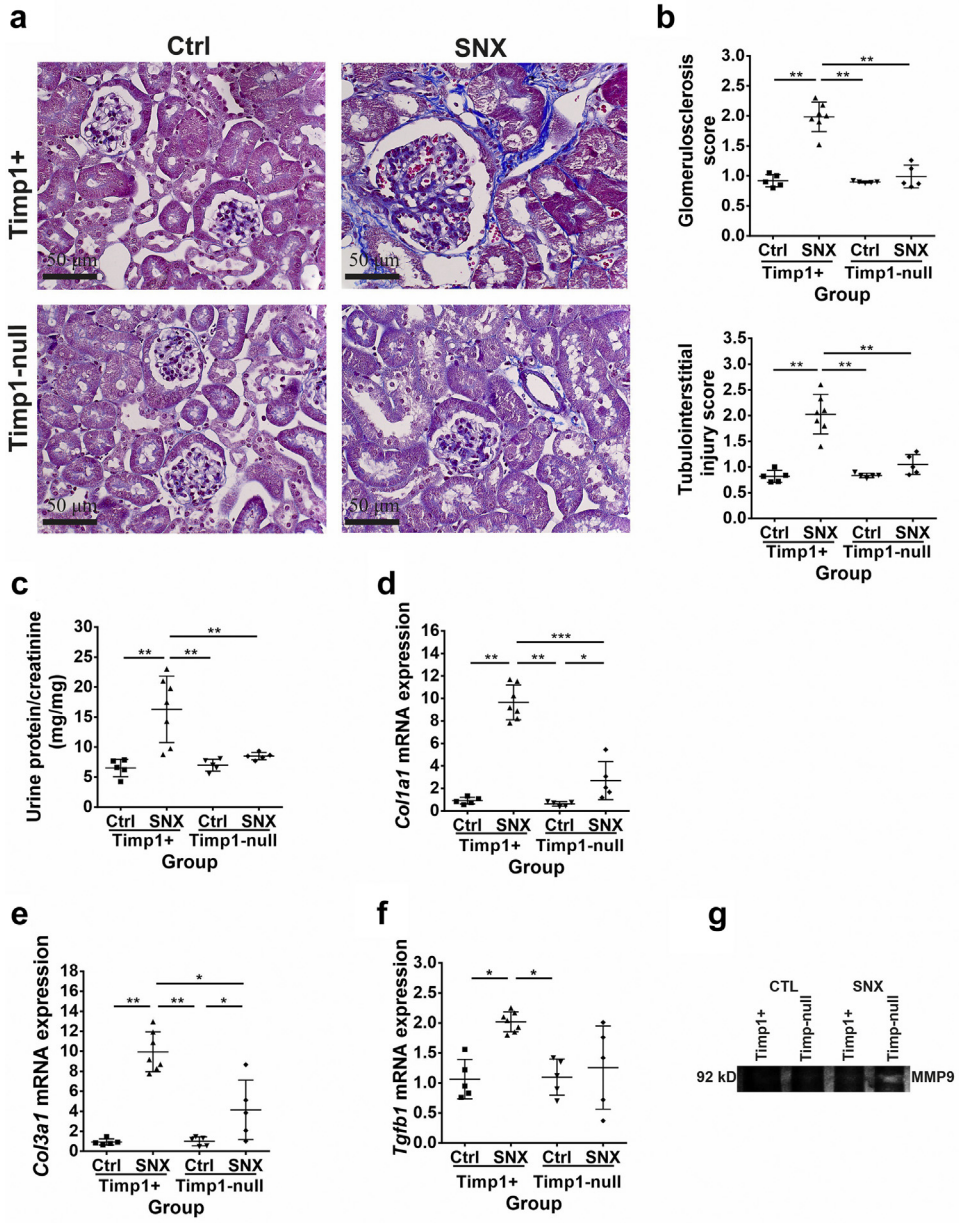

Figure 8 | Subtotal renal ablation (SNX) in Timp1-null mice. (**a,b**) SNX in Timp1-null male mice on the fibrosis-prone CBAxB6 F1 genetic background induced only minor glomerular or tubulointerstitial changes, compared with significant glomerular scarring and interstitial fibrosis in Timp1+ (wild-type) control CBAxB6 F1 mice. Timp1-null SNX mice (**c**) did not develop proteinuria and (**d,e**) only mild overexpression of type-I (*Col1a1*) and type-III collagen (*Col3a1*) mRNA overexpression, compared with the Timp1+ SNX control mice with 2-fold higher proteinuria and 3-fold higher renal collagen overexpression. (**f**) Of note, renal transforming growth factor-beta1 (TGF-β_1) mRNA (*Tgfb1*) expression was similar to that in controls in Timp1-null SNX kidneys, despite the 2-fold overexpression in wild-type SNX kidneys. (**g**) Representative photo of matrix metalloproteinase-9 (MMP9) gelatinase activity shows a visible band only in Timp1-null SNX. All data are presented as fold expression to control (Ctrl) sample (mean ± SD; n = 5–7/group). Masson's trichrome stain; bar = 50 μm. Kruskal-Wallis test, *$P < 0.05$; **$P < 0.01$; ***$P < 0.001$. To optimize viewing of this image, please see the online version of this article at www.kidney-international.org.

Figure 7 | (continued) (*Lcn2*) mRNA, as well as (**g**) significant tissue inhibitor of matrix metalloproteinase-1 (TIMP-1) mRNA (*Timp1*) and protein overexpression, accompanied by (**i**) *Egr2* mRNA, compared with B6 SNX and controls (Ctrl). (**h**) Immunostaining showed significant co-localization of tubular TIMP1 and early growth response factor-2 (EGR2) in CBA SNX kidneys and an increased number of interstitial EGR2-positive cells (arrows; EGR2: red; TIMP1: green; EGR2 + TIMP1: yellow; 4′,6-diamidino-2-phenylindole [DAPI]: blue, nuclear stain; bar = 50 μm). All data are presented as fold expression to control sample (mean ± SD, n = 4/group). Kruskal-Wallis test, *$P < 0.05$; **$P < 0.01$. g, glomerulus. To optimize viewing of this image, please see the online version of this article at www.kidney-international.org.

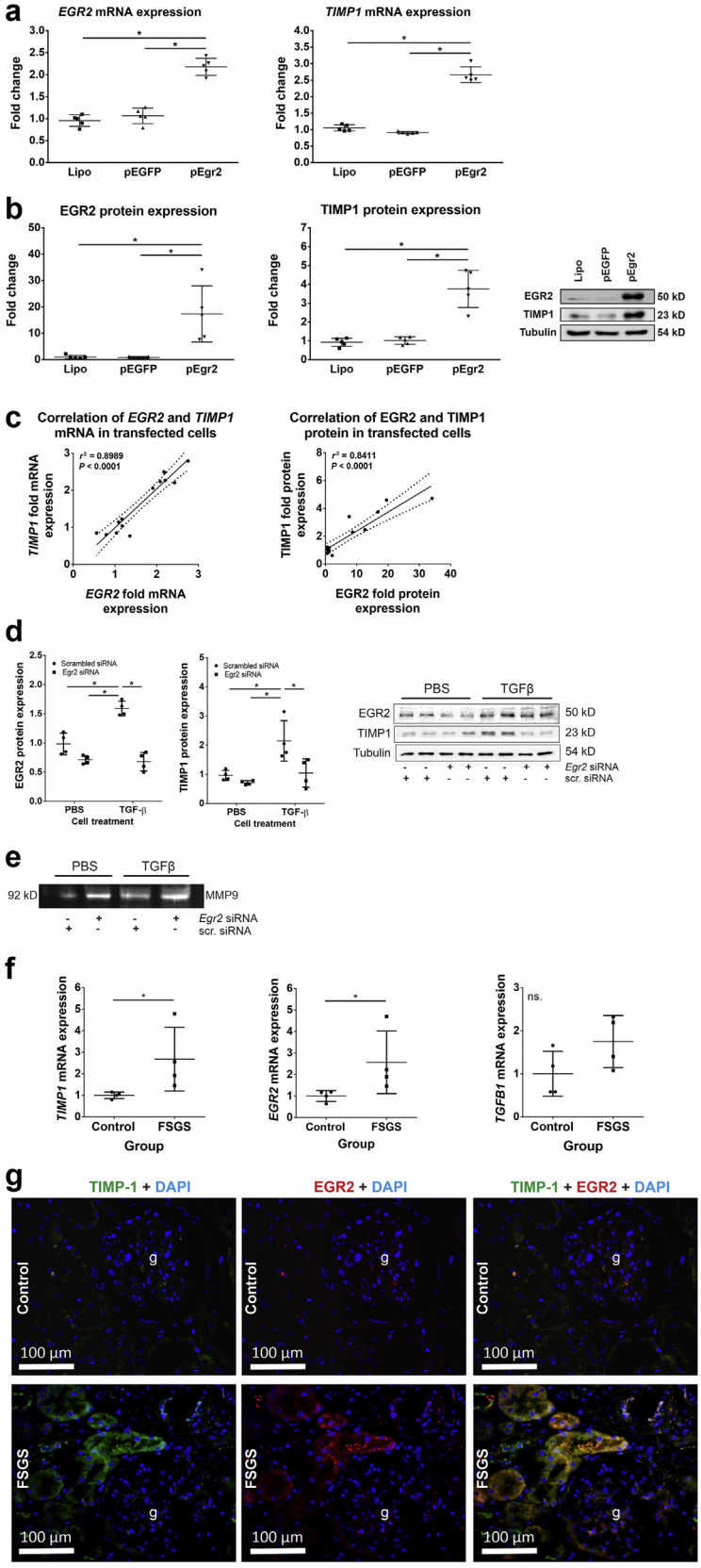

Figure 9 | The effect of early growth response factor-2 (EGR2) overexpression in cultured human embryonic kidney (HEK)293 cells and EGR2 expression in human focal segmental glomerular sclerosis (FSGS). HEK293 cells were transiently transfected with pCMV plasmid containing full length *Egr2* gene (pEGR2; $n = 5$) or *EGFP* (pEGFP; $n = 5$), and nontransfected negative controls (Ctrl) were treated with (continued)

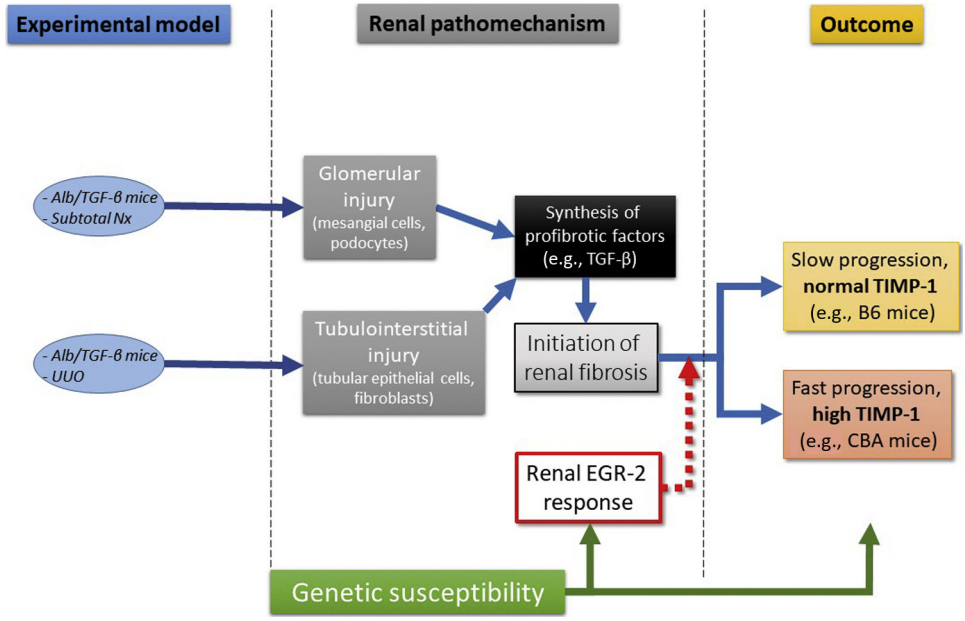

Figure 10 | Proposed effect of genetically determined renal fibrosis progression in mice. In our experiments, we confirmed the importance of genetically determined renal tissue inhibitor of matrix metalloproteinase-1 (TIMP-1) response in experimental models of both glomerular and tubulointerstitial injury. The elevated circulating transforming growth factor-beta1 (TGF-β_1) levels of Alb/TGF-β_1 transgenic mice induce glomerulosclerosis and tubulointerstitial fibrosis. Subtotal nephrectomy (Nx) leads to glomerular hyperfiltration in the remnant nephrons, inducing glomerulosclerosis. Unilateral ureter obstruction (UUO) causes tubular injury and dilatation, mainly leading to interstitial fibrosis. Regardless of glomerular or tubulointerstitial injury, the consecutive renal synthesis of TGF-β_1 and other profibrotic factors initiate the kidney scarring processes. We propose that the genetically determined early growth response factor-2 (EGR2) response in the kidneys influences the progression rate of the initiated fibrosis. The outcome will be either slow progression due to normal or mildly elevated EGR2 and TIMP-1 levels (e.g., in fibrosis-resistant B6 mice) or alternatively, fast fibrosis progression due to high EGR2 and TIMP-1 expression in the kidneys (e.g., in fibrosis-prone CBA mice) influenced by genetic susceptibility. Therefore, this renal EGR2-TIMP-1 response might play a major role in the outcome of fibrosis.

obstructive uropathy.[29] However, this raises the question of whether the TIMP-1 overexpression in CBAxB6-TGFβ mice is a component of the excessive scarring, or whether the upregulated TIMP-1 has a causal role in the development of fibrosis in this TGF-β1–transgenic model.

Therefore, we analyzed mice at age 5 days, when CBAxB6-TGFβ1 kidneys exhibited only mild glomerular hypertrophy, and in approximately 30% of glomeruli, slight mesangial expansion. Even at this early age, EGR2 and TIMP-1 were significantly upregulated in CBAxB6-TGFβ mice, compared with B6-TGFβ mice (Figure 4d and e; Supplementary Figure S5), accompanied by elevated renal *Tgfb1* mRNA, but not collagen overexpression. The comparable renal *Egr2* and *Timp1* mRNA expression in newborn TGFβ1-transgenic mice indicates that the differences in renal fibrosis progression were not a consequence of increased perinatal EGR2 or TIMP-1 expression. Taken together, these results demonstrate that early induction of renal EGR2 and TIMP-1 in CBAxB6-TGFβ mice precedes the overproduction of extracellular matrix components, and the TIMP-1–driven inhibition of MMP9 activity contributes to extracellular matrix accumulation. Administration of neutralizing TIMP-1 antibody ameliorated the potent profibrotic effect of TGFβ1 in CBAxB6-TGFβ kidneys, and it reduced fibrosis, proteinuria, and serum urea levels (Figure 5), supporting the important role of TIMP-1 in promoting renal scarring.

Figure 9 | (continued) Lipofectamine (Lipo; $n = 5$). Transfection for 24 hours with pEGR2 increased the expression of (**a**) *EGR2* mRNA and *TIMP1* mRNA, and (**b**) EGR2 and tissue inhibitor of matrix metalloproteinase-1 (TIMP1) protein. Representative immunoblots for EGR2 and TIMP1 are also shown. (**c**) Furthermore, EGR2 correlated tightly with TIMP-1 at both the mRNA level ($n = 15$) and the protein level ($n = 12$). In human kidney (HK)–2 cells, transfection with *EGR2* small, interfering (si)RNA 1 days prior to transforming growth factor-beta (TGF-β) treatment basically inhibited the TGF-β–induced EGR2 and TIMP1 production, compared with (**d**) scrambled siRNA-treated cells. (**e**) This reduced TIMP1 resulted in elevated matrix metalloproteinase-9 (MMP9) gelatinase activity, as shown by representative zymogram performed from conditioned cell media. Additionally, kidney cortex biopsies of FSGS patients ($n = 4$) were compared to control kidney samples (extracted from healthy cortex area of nephrectomized tissues, due to renal cancer, $n = 4$). (**f**) FSGS samples showed significantly higher *EGR2* and *TIMP1* mRNA expression, compared with controls, but only tendentially increased *TGFB1* mRNA. (**g**) Immunostaining of FSGS biopsies revealed a marked (green) tubular TIMP1 expression, compared with control samples, accompanied by (red) increased interstitial and tubular EGR2 expression that largely co-localized with (yellow) TIMP1. Bar = 100 μm. All data are presented as fold expression compared to control sample (mean ± SD), Kruskal-Wallis or Mann-Whitney test were performed, and 2-way analysis of variance for gene silencing study, $^*P < 0.05$. DAPI, 4′,6-diamidino-2-phenylindole; g, glomerulus; PBS, phosphate-buffered saline. To optimize viewing of this image, please see the online version of this article at www.kidney-international.org.

Transgenic mouse models often raise the question of whether the observations are unique consequences of the transgene, acting in the mouse context itself, or whether they might lead to broader understanding of human pathophysiology. UUO and SNX are widely used experimental models of kidney fibrosis. UUO causes tubulointerstitial damage that usually leads to fibrosis within 7 days,[17] and SNX causes hyperfiltration in the remnant glomeruli and leads to glomerulosclerosis with concomitant interstitial fibrosis within usually 15–20 weeks.[30] Based on the results of our TGF-β1–transgenic mice, we investigated how genetic background influences the early events of fibrosis within 24 hours and 6 weeks in UUO and SNX models, respectively. Both UUO and SNX performed on wild-type B6 and CBA mice lead to early renal EGR2 and TIMP-1 induction in the susceptible CBA strain (Figures 6 and 7). Thus, genetic susceptibility to kidney fibrosis was strongly associated with EGR2 and TIMP-1 not only in the TGF-β1–transgenic model, but also after UUO or SNX. Our comparison of Timp1-null and Timp1+ control male mice subjected to SNX further supports the central role of TIMP-1 in the pathogenesis of renal fibrosis (Figure 8). Interestingly, a similar fibrosis rate was previously reported in TIMP-1–deficient and control mice 14 days after UUO,[31] but that study used a different, 129Sv mouse strain. Moreover, the very late (14 days) evaluation time point in that study is partly in line with our observation that, despite the early differences at 24 hours after UUO in B6 and CBA males, basically similar fibrosis developed at a later stage (7 days), although the MMP9 gelatinase activity was still higher in B6 UUO mice than in CBA UUO mice, even at 7 days. To overcome the limitations of the UUO model that relate to hydronephrosis, we utilized the SNX model as well, which more closely resembles human kidney fibrosis development than does the UUO model.

Additionally, overexpressing EGR2 *in vitro* induced TIMP1 protein of HEK293 cells, and TIMP1 was correlated to EGR2 (Figure 9), whereas *EGR2* silencing in HK-2 cells inhibited the TGF-β1–induced EGR2 and TIMP1 overproduction, resulting in higher MMP9 activity. Moreover, *Egr2* silencing *in vivo* markedly reduced the UUO-induced EGR2 and TIMP1 overexpression in mice. Of note, expression in kidney biopsies from FSGS patients supported our *in vitro* and *in vivo* results. These data suggest a novel role for the transcription factor EGR2 in renal fibrogenesis.

In conclusion, our studies demonstrate that genetic background has a significant impact on the effect of TGF-β1, a potent profibrotic cytokine. Genetic background influences early renal EGR2 and TIMP-1 expression that regulates MMP9 activity, which is associated with resistance (B6 background) or susceptibility (CBA background) to fibrosis progression in mice, suggesting that EGR2 and TIMP-1 play an important role in the initiation of fibrosis (Figure 10). Still, further studies are needed to clarify how the genetic background of mice influences the early renal EGR2 response to injury (e.g., via altered microRNA or long, noncoding RNA) and whether EGR2 has a direct or indirect effect on TIMP1.

DISCLOSURE

All the authors declared no competing interests.

DATA STATEMENT

Microarray data of this study are openly available in repository (National Center for Biotechnology Information Gene Expression Omnibus, GSE54441) at the following URL: https://www.ncbi.nlm.nih.gov/geo.

ACKNOWLEDGMENTS

Financial support was provided by grants from the Hungarian Scientific Research Fund (OTKA PD 112960 to GK), the Hungarian Society for Hypertension Scientific Grant (to GK), the STIA-OTKA Grant of the Semmelweis University Innovation Center (137266/TMI/2020), the Bolyai Scholarship of the Hungarian Academy of Sciences (BO/00304/20/5 to GK), the ÚNKP Bolyai+ Scholarship from the Hungarian Ministry of Innovation and Technology and the National Research, Development and Innovation Office (to GK) and the NIDDK Intramural Research Program (to JBK).

The authors thank the following for their valuable technical assistance: Krisztina Fazekas (Semmelweis University, Institute of Translational Medicine), Ágnes Udri, Ildikó Virág (GMO Animal Facility of Semmelweis University), Magdolna Pekár and Erzsébet Kovács (2nd Department of Pathology, Semmelweis University), as well as Dr. Attila Fintha (1st Department of Pathology, Semmelweis University) and Magdolna Kardos (2nd Department of Pathology) for their help with human kidney samples. The authors also acknowledge support from NIDDK Microarray Core facility (National Institutes of Health [NIH], USA).

SUPPLEMENTARY MATERIAL

Supplementary File (Word)

Supplementary Methods.

Supplementary References.

Figure S1. (**A**) Overview of breeding strategy for transforming growth factor-beta (TGF-β) transgenic strains. Backcross of transforming growth factor-beta1 (TGF-β1) transgenic mice to CBA strain failed due to premature death, whereas continuous backcrosses to B6 strain over 22 generations resulted in congenic B6-alb/TGFβ (B6-TGFβ) transgenic male mice with 99.9% homogeneous genetic background. Novel F1 transgenic mice were then generated by crossing B6-TGFβ males and CBA females, resulting in CBAxB6-TGFβ F1 transgenic males with very short survival time due to uremia. (**B**) Histopathologic findings in B6 wild-type and B6-TGFβ transgenic mice at the age of 4 months and 9 months, respectively. Only B6-TGFβ mice had glomerular enlargement and mild mesangial expansion at both time points. Masson's trichrome stain, original magnification ×400. Bar = 50 μm.

Figure S2. (**A**) Representative immunoblot of *SMAD3* protein phosphorylation in the kidneys of transforming growth factor-beta (TGF-β) transgenic mice and wild-type controls at age 14 days, depicting similar *SMAD3* activity in all mouse strains ($n = 3$/group). (**B**) Liver samples of 14-day-old mice were stained according to van Gieson, and the percentage of connective tissue per area was calculated using ImagePro software. (**C**) The hepatic expression of TGF-β transgene resulted in slight liver fibrosis as compared to controls, but there was no difference between transgenic strains ($n = 7$–14/group). In order to analyze possible strain-dependent cardiac

effects of the elevated plasma TGF-β levels, myocardial *Col1a1* mRNA expression was analyzed but revealed no significant difference among the strains regardless of TGF-β levels at the age of 14 days ($n = 5$–6/group). Kruskal-Wallis test, $^*P < 0.05$.

Figure S3. Heat map clustering of significantly altered top 311 genes in CBAxB6–transforming growth factor-beta (TGFβ) versus B6-TGFβ transgenic mouse kidneys (>2-fold [log2] expression changes; blue shows downregulation, red shows upregulation).

Figure S4. Top 70 kidney disease–related genes with altered expression in CBAxB6–transforming growth factor-beta (TGFβ) versus B6-TGFβ transgenic mouse kidneys were obtained by enrichment analysis of array data (Thomson Reuters Metacore; *Timp1* is marked with red).

Figure S5. Early growth response factor-2 (EGR2) and tissue inhibitor of matrix metalloproteinase-1 (TIMP1) protein expression in the kidneys of transforming growth factor-beta (TGF-β) transgenic mice and wild-type controls at the age of 5 days. (**A**) Evaluation of EGR2 immunoreactivity (**B**, yellow) showed higher expression in CBAxB6-TGFβ kidneys as early as at 5 days of age, showing colocalization with TIMP1 in tubules. Although EGR2-positive interstitial cells (red/pink, see arrows) appeared in both B6-TGFβ and CBAxB6-TGFβ kidneys, tubular EGR2 and significant TIMP1 expression appeared in only the CBAxB6-TGFβ mice. Representative photomicrographs at original magnification ×400 ($n =$ 4/group, bar = 50 μm, g, glomerulus, TIMP1 [green], EGR [red], 4′,6-diamidino-2-phenylindole [DAPI; blue, nuclear stain]).

Figure S6. Early growth response factor-2 (EGR2) protein expression in kidneys of B6 and CBA mice 24 hours after unilateral ureter obstruction (UUO). Representative photomicrographs of immunostaining at original magnification ×400 (**A**) depict a few interstitial nuclear EGR2 (pink)-positive cells (arrows) in controls that increased mildly in B6 UUO accompanied by light tubular staining. However, EGR2 positivity increased significantly in CBA UUO kidneys, not only as an increased number of interstitial cells (arrows) but also as more prominent tubular EGR2 staining (asterisks). (**B**) Evaluation of the EGR2 immunostaining revealed significantly higher EGR2 expression in CBA UUO kidneys ($n = 4$/group, Kruskal-Wallis test, $^*P < 0.05$; bar = 50 μm, g, glomerulus, EGR2 [red] and 4′,6-diamidino-2-phenylindole [DAPI; blue, nuclear stain]).

Figure S7. Strain-related renal differences 7 days after unilateral ureter obstruction (UUO). (**A**) Seven days after UUO in both B6 and CBA male mice, we observed significant interstitial fibrosis with marked tubular dilation and tubular epithelial atrophy, which was more prominent in CBA UUO kidneys. (**B**) This was accompanied by higher *Timp1* mRNA expression in CBA UUO ($n = 5$/group) but (**C**) only mildly higher (not significant) *Egr2* expression as compared to B6 UUO. (**D**) Matrix metalloproteinase-9 (MMP9) gelatinase activity was reduced in CBA UUO kidneys as compared to B6 UUO. Expression of each mRNA was normalized to 18S rRNA (Rn18s) using the $2^{-\Delta\Delta Ct}$ formula. All data are presented as fold expression compared to control sample (mean ± SD). Kruskal-Wallis test, $^*P <$ 0.05. Masson's trichrome stain, original magnification ×400. Bar = 50 μm.

Figure S8. Early growth response factor-2 (EGR2) protein expression in kidneys of B6 and CBA mice 6 weeks after subtotal renal ablation (SNX). (**A**) Representative photomicrographs at original magnification ×400 show scarce EGR2 (red) positivity (arrows) in controls, and a mild increase in B6 SNX, but significantly increased EGR2 positivity in CBA SNX kidneys, where interstitial EGR2-positive cells (pink) also appear (asterisks). (**B**) Evaluation of the EGR2 immunostaining revealed markedly higher EGR2 expression in CBA SNX kidneys ($n = 4$/group, Kruskal-Wallis test, $^*P < 0.05$; bar = 50 μm, g, glomerulus, EGR2 [red] and 4′,6-diamidino-2-phenylindole [DAPI; blue, nuclear stain]).

Figure S9. Tissue inhibitor of matrix metalloproteinase-1 (TIMP1) and early growth response factor-2 (EGR2) mRNA expression in human fibroblasts (HFF-1) after transforming growth factor-beta (TGF-β) treatment *in vitro*. (**A**) Treatment of human foreskin fibroblast cells with 10 ng/ml TGF-β for 24 h resulted in markedly increased TIMP1 and (**B**) EGR2 mRNA expression as compared to phosphate-buffered saline (PBS)–treated cells ($n = 4$/group, Kruskal-Wallis test, $^*P < 0.05$).

Figure S10. Effect of *in vivo* early growth response factor-2 (EGR2) gene silencing on EGR2 and tissue inhibitor of matrix metalloproteinase-1 (TIMP1) expression 24 hours after unilateral ureter obstruction (UUO). (**A**) EGR2 small, interfering RNA administration 24 hours prior to UUO ($n = 4$) significantly lowered the UUO-induced *Egr2* mRNA overexpression by 50%, accompanied by similar reduced *Timp1* mRNA as compared to scrambled siRNA-treated mice ($n = 5$). (**B**) Immunostaining revealed increased tubular TIMP-1 (green) expression in scrambled siRNA-treated UUO kidneys with EGR2 co-localization (yellow) in some tubules, accompanied by several EGR2-positive interstitial cells (pink, see arrows). In contrast, EGR2 siRNA-treated UUO kidneys revealed markedly less TIMP-1 and EGR2 staining, with reduced interstitial EGR2 positivity. Contralateral kidneys as controls were minimally TIMP-1 positive with only a few interstitial EGR2 positive cells. Representative photomicrographs at original magnification ×400 (bar = 100 μm, TIMP1 [green], EGR [red], 4′,6-diamidino-2-phenylindole [DAPI; blue, nuclear stain]; Kruskal-Wallis test, $^*P < 0.05$).

Table S1. Laboratory and pathology data of B6–transforming growth factor-beta (TGFβ) transgenic and wild-type control mice at ages 4 months and 9 months.

Table S2. Antibodies used for immunohistochemistry and immunoblotting.

Table S3. Mouse and human primer sequences (5′–3′) used for quantitative PCR.

Table S4. Top 10 altered process networks and affected genes in CBAxB6–transforming growth factor-beta (TGFβ) versus B6-TGFβ mouse kidneys at the age of 14 days. FDR, false discovery rate.

Table S5. qPCR validation of selected genes from array data.

Table S6. qPCR validation of transcription factors from array data.

Table S7. Basic data on human kidney sample pathology in renal cortex biopsies (focal segmental glomerulosclerosis [FSGS] group) or nephrectomy samples (control group) analyzed for mRNA expression. For the control samples, only healthy renal cortex was excised for RNA isolation.

REFERENCES

1. Keith DS, Nichols GA, Gullion CM, et al. Longitudinal follow-up and outcomes among a population with chronic kidney disease in a large managed care organization. *Arch Intern Med*. 2004;164:659–663.
2. August P, Suthanthiran M. Transforming growth factor beta and progression of renal disease. *Kidney Int Suppl*. 2003;(87):S99–S104.
3. Khan R. Examining potential therapies targeting myocardial fibrosis through the inhibition of transforming growth factor-beta 1. *Cardiology*. 2007;108:368–380.
4. Murray LA, Chen Q, Kramer MS, et al. TGF-beta driven lung fibrosis is macrophage dependent and blocked by serum amyloid P. *Int J Biochem Cell Biol*. 2011;43:154–162.
5. Kökény G, Németh Z, Godó M, Hamar P. The Rowett rat strain is resistant to renal fibrosis. *Nephrol Dial Transplant*. 2010;25:1458–1462.
6. Grond J, Beukers JY, Schilthuis MS, et al. Analysis of renal structural and functional features in two rat strains with a different susceptibility to glomerular sclerosis. *Lab Invest*. 1986;54:77–83.
7. Grond J, Muller EW, van Goor H, et al. Differences in puromycin aminonucleoside nephrosis in two rat strains. *Kidney Int*. 1988;33:524–529.
8. Chen JS, Chen A, Chang LC, et al. Mouse model of membranous nephropathy induced by cationic bovine serum albumin: antigen

dose-response relations and strain differences. *Nephrol Dial Transplant*. 2004;19:2721–2728.
9. Ishola DA Jr, van der Giezen DM, Hahnel B, et al. In mice, proteinuria and renal inflammatory responses to albumin overload are strain-dependent. *Nephrol Dial Transplant*. 2006;21:591–597.
10. Ma LJ, Fogo AB. Model of robust induction of glomerulosclerosis in mice: importance of genetic background. *Kidney Int*. 2003;64:350–355.
11. Salzler HR, Griffiths R, Ruiz P, et al. Hypertension and albuminuria in chronic kidney disease mapped to a mouse chromosome 11 locus. *Kidney Int*. 2007;72:1226–1232.
12. Gurley SB, Clare SE, Snow KP, et al. Impact of genetic background on nephropathy in diabetic mice. *Am J Physiol Renal Physiol*. 2006;290:F214–F222.
13. Rumberger B, Vonend O, Kreutz C, et al. cDNA microarray analysis of adaptive changes after renal ablation in a sclerosis-resistant mouse strain. *Kidney Blood Press Res*. 2007;30:377–387.
14. Sanderson N, Factor V, Nagy P, et al. Hepatic expression of mature transforming growth factor beta 1 in transgenic mice results in multiple tissue lesions. *Proc Natl Acad Sci U S A*. 1995;92:2572–2576.
15. Mozes MM, Bottinger EP, Jacot TA, et al. Renal expression of fibrotic matrix proteins and of transforming growth factor-beta (TGF-beta) isoforms in TGF-beta transgenic mice. *J Am Soc Nephrol*. 1999;10:271–280.
16. Fang F, Ooka K, Bhattacharyya S, et al. The early growth response gene Egr2 (Alias Krox20) is a novel transcriptional target of transforming growth factor-beta that is up-regulated in systemic sclerosis and mediates profibrotic responses. *Am J Pathol*. 2011;178:2077–2090.
17. Klahr S, Morrissey J. Obstructive nephropathy and renal fibrosis. *Am J Physiol Renal Physiol*. 2002;283:F861–F875.
18. Border WA, Noble NA, Yamamoto T, et al. Natural inhibitor of transforming growth factor-beta protects against scarring in experimental kidney disease. *Nature*. 1992;360:361–364.
19. Hildebrand A, Romaris M, Rasmussen LM, et al. Interaction of the small interstitial proteoglycans biglycan, decorin and fibromodulin with transforming growth factor beta. *Biochem J*. 1994;302(Pt 2):527–534.
20. Poncelet AC, de Caestecker MP, Schnaper HW. The transforming growth factor-beta/SMAD signaling pathway is present and functional in human mesangial cells. *Kidney Int*. 1999;56:1354–1365.
21. Seeland U, Haeuseler C, Hinrichs R, et al. Myocardial fibrosis in transforming growth factor-beta(1) (TGF-beta(1)) transgenic mice is associated with inhibition of interstitial collagenase. *Eur J Clin Invest*. 2002;32:295–303.
22. Allan JA, Docherty AJ, Barker PJ, et al. Binding of gelatinases A and B to type-I collagen and other matrix components. *Biochem J*. 1995;309(Pt 1):299–306.
23. Olson MW, Toth M, Gervasi DC, et al. High affinity binding of latent matrix metalloproteinase-9 to the alpha2(IV) chain of collagen IV. *J BiolChem*. 1998;273:10672–10681.
24. Vollmann EH, Cao L, Amatucci A, et al. Identification of novel fibrosis modifiers by in vivo siRNA silencing. *Mol Ther Nucleic Acids*. 2017;7:314–323.
25. Suzuki D, Miyazaki M, Jinde K, et al. In situ hybridization studies of matrix metalloproteinase-3, tissue inhibitor of metalloproteinase-1 and type IV collagen in diabetic nephropathy. *Kidney Int*. 1997;52:111–119.
26. Sanders JS, van Goor H, Hanemaaijer R, et al. Renal expression of matrix metalloproteinases in human ANCA-associated glomerulonephritis. *Nephrol Dial Transplant*. 2004;19:1412–1419.
27. Nakamura T, Ebihara I, Tomino Y, et al. Effect of a specific endothelin A receptor antagonist on murine lupus nephritis. *Kidney Int*. 1995;47:481–489.
28. Eddy AA. Molecular insights into renal interstitial fibrosis. *J Am Soc Nephrol*. 1996;7:2495–2508.
29. Sharma AK, Mauer SM, Kim Y, et al. Altered expression of matrix metalloproteinase-2, TIMP, and TIMP-2 in obstructive nephropathy. *J Lab Clin Med*. 1995;125:754–761.
30. Shimamura T, Morrison AB. A progressive glomerulosclerosis occurring in partial five-sixths nephrectomized rats. *Am J Pathol*. 1975;79:95–106.
31. Kim H, Oda T, Lopez-Guisa J, et al. TIMP-1 deficiency does not attenuate interstitial fibrosis in obstructive nephropathy. *J Am Soc Nephrol*. 2001;12:736–748.